

Formation of Ductile Amorphous & Nanocrystalline Ni-W Alloys by Electrodeposition

By T. Yamasaki, R. Tomohira, Y. Ogino, P. Schloßmacher & K. Ehrlich

Amorphous and nanocrystalline Ni-W alloys having both high hardness and high ductility were prepared by electrodeposition. The plating bath for the electrodeposition contained nickel sulfate, trisodium citrate, sodium tungstate and ammonium chloride, and was operated at various bath concentrations and conditions of electrolysis. The tungsten content of the Ni-W electrodeposits is influenced by the plating bath temperature and the applied current density. An amorphous phase appeared at a tungsten content of more than about 20 atomic pct. The ductility of the electrodeposited alloys is strongly influenced by the plating bath temperature, especially the highly ductile amorphous and nanocrystalline Ni-W alloys containing between 17.7 and 22.5 at pct W. They have been obtained at a plating bath temperature of 75 °C: bending through an angle of 180° is possible without breaking. It is suggested that the ductility of the Ni-W electrodeposited alloys may be strongly influenced by inclusion of the codeposited hydrogen during the electrodeposition process.

Electrodeposition of alloys is particularly important for applications to microfabrication technologies, especially to the molding process of LIGA technology that requires hard microstructures. Electrodeposited alloys having high hardness, however, are generally limited in these applications because of their brittleness.¹

Amorphous and nanocrystalline electrodeposited Ni-W alloys have some excellent properties, such as high hardness, high corrosion resistance and high thermal stability. The process for electrodeposition of W-rich Ni-W alloys, however, has not yet been well developed and the electrodeposited alloys have been severely brittle.¹⁻⁵ In our previous study, we developed an aqueous plating bath for Ni-W

electrodeposition that yields amorphous alloys of fairly high tungsten content.⁶⁻⁸ In this study, the electroplating conditions for producing the ductile amorphous and nanocrystalline Ni-W alloys have been investigated in detail. Our purpose is to show that Ni-W alloys having both high hardness and high ductility can be produced by electrodeposition if experimental parameters are carefully chosen.

Experimental Procedure

The plating bath composition and conditions selected for this study are shown in Table 1. Trisodium citrate and ammonium chloride were introduced as complexing agents to form complexes with both Ni and W in the plating bath solution. To improve conductivity, sodium bromide was used. Electrodeposition was done using Cu sheets as substrates prepared by electropolishing; a high-purity platinum sheet was used as the anode. The plating cells (600-mL beakers, each containing 500 mL of the bath) were controlled by a thermostat to maintain the desired bath temperature. A fresh plating bath was made for each experiment, using analytical reagent grade chemicals and deionized water. The deposition rate of the Ni-W alloys was determined by weighing the substrate before

Table 1
Plating Bath Composition & Conditions for Ni-W Electrodeposition

Nickel sulfate, NiSO ₄ · 6H ₂ O	0.06 mol/L
Trisodium citrate, Na ₃ C ₆ H ₅ O ₇ · 2H ₂ O	0.3 ~ 0.5 mol/L
Sodium tungstate, Na ₂ WO ₄ · 2H ₂ O	0.14 mol/L
Ammonium chloride, NH ₄ Cl	0.5 mol/L
Sodium bromide, NaBr	0.15 mol/L
Bath temperature	60 ~ 90 °C
pH	8.5
Current density	0.05 ~ 0.2 A/dm ²

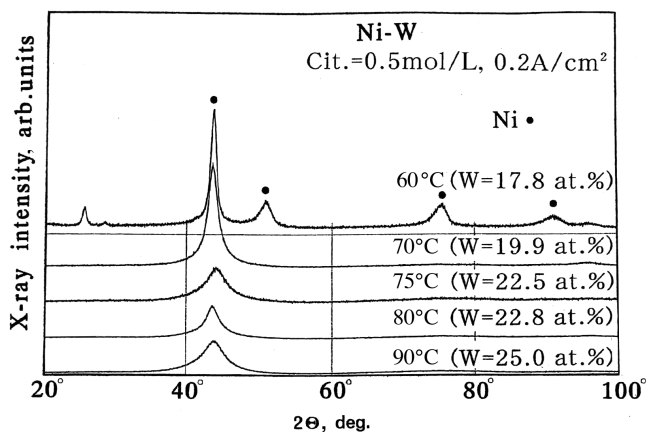


Fig. 1—X-ray diffraction patterns of electrodeposited Ni-W alloys for various plating bath temperatures at a current density of 0.2 A/cm².

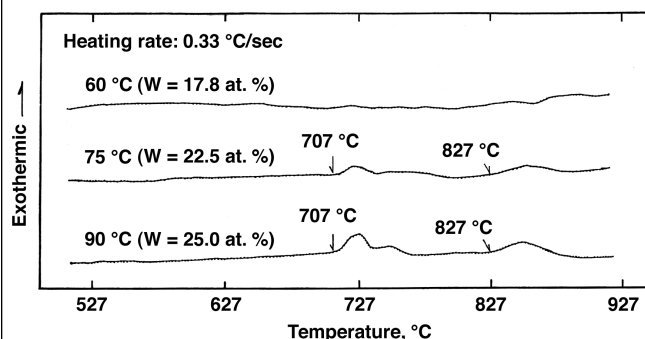


Fig. 2—DTA thermograms of electrodeposited Ni-W alloys for various plating bath temperatures at a heating rate of 0.33 °C/sec.

and after the one-hr electrodeposition and calculating the additional mass per square centimeter. The electrodeposited Ni-W films were separated from the Cu substrates by immersing the samples in an aqueous solution containing CrO_3 (250 g/L) and H_2SO_4 (15 cc/L).

Structural analysis of the electrodeposited alloys was performed by means of X-ray diffraction using Cu-K α radiation (rotating anode type X-ray apparatus, 40 kV-200 mA) and high-resolution transmission electron microscopy (HR-TEM, 200 kV). Elemental concentrations of the electrodeposits were analyzed by wavelength-crystal dispersion X-ray spectroscopy (WDS) in a scanning electron microscope. The samples prepared were annealed at various temperatures in vacuum of about 10^{-3} Pa. The degree of ductility was determined by measuring the radius of curvature at which the fracture occurred in a simple bending test. The fracture strain on the outer surface of the specimen, ϵ_f , is estimated by the equation, $\epsilon_f = t/(2r-t)$, where r is the radius of curvature on the outer surface of the bend sample at the fracture and t is the thickness of the specimen. Vickers microhardness was measured by using the as-deposited and the annealed samples on Cu substrates with a 0.02 kg load and a loading time of 15 sec in cross section.

Results

Formation of Ductile Ni-W Electrodeposits Plating bath temperature

The tungsten content of the electrodeposits is strongly influenced by the plating bath temperature. Figure 1 shows the X-

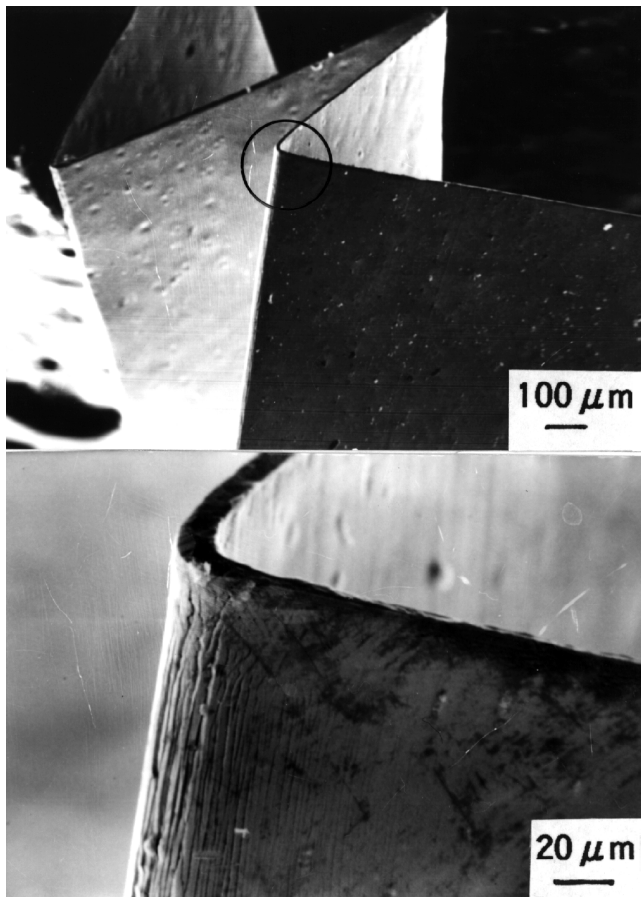


Fig. 3—SEM micrographs of as-deposited Ni-22.5 at pct W alloys at a plating bath temperature of 75 °C after bending through an angle of 180°. They deform plastically and extremely non-homogeneously: shear bands form on the bending edge.

ray diffraction patterns of the Ni-W electrodeposits and their tungsten contents for various plating bath temperatures between 60 and 90 °C at the applied current density of 0.2 A/cm². The tungsten content of the electrodeposits increased with increasing plating bath temperature and the amorphous pattern appeared at a tungsten content of about 20 at pct or more. Figure 2 shows DTA measurements at a heating rate of 0.33 °C/sec of the as-deposited Ni-W alloys for various plating bath temperatures. No distinct crystallization peaks were observed for the Ni-17.8 at pct W alloy electrodeposited at a plating bath temperature of 60 °C. At a bath temperature of 75 °C and above, the amorphous X-ray diffraction pattern appeared with the crystallization of these amorphous Ni-W alloys taking place in two steps. The first step, starting at a temperature of about 707 °C has been confirmed by X-ray analysis to result from crystallization of the fcc Ni-W solid solution. The second step of the DTA thermograms takes place at a temperature range from 827 to 877 °C. X-ray analysis has suggested that Ni₄W intermetallic compound precipitates during this step.

Deposition rate and mechanical properties vs. plating bath temperature for the Ni-W electrodeposits are shown in Table 2. The Vickers microhardness of the electrodeposits increased continuously from 602 to 770 with increasing plating bath temperature, from 60 to 90 °C, respectively. The deposition rate reached its maximum value of 68.8 mg/cm² · hr at a plating bath temperature of 75 °C, then decreased with increasing plating bath temperature. It may be noted that the as-electrodeposited Ni-22.5 at pct W alloy at the plating bath temperature of 75 °C and having high hardness of HV = 685 was ductile: it could be bent through an angle of 180° without breaking ($\epsilon_f = 1.0$). At other plating bath temperatures, the electrodeposits were severely brittle. Figure 3 shows SEM micrographs of the Ni-22.5 at pct W alloys electrodeposited at 75 °C after bending through an angle of 180°. They deform plastically and extremely non-homogeneously: shear bands form on the bending edge, showing the typical feature of the ductile metallic glasses.

Applied current density

The tungsten content of the Ni-W electrodeposits is also influenced by the applied current density. Figure 4 shows X-ray diffraction patterns of as-deposited Ni-W alloys for

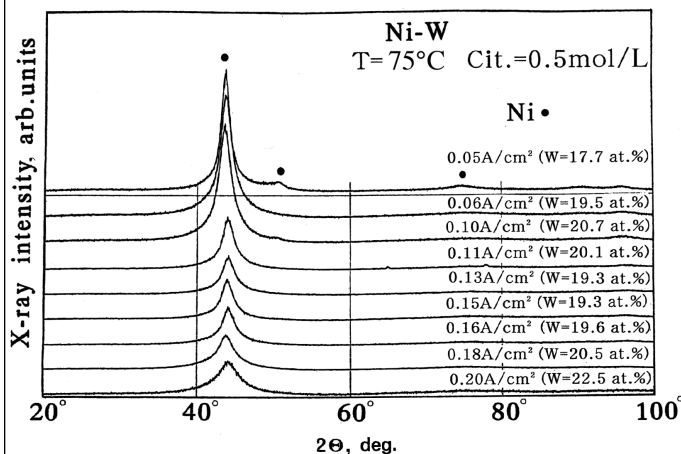


Fig. 4—X-ray diffraction patterns of as-deposited Ni-W alloys for various current densities between 0.05 and 0.2 A/cm² at the plating bath temperature of 75 °C. All of these Ni-W alloys are ductile: they can be bent through an angle of 180° without breaking.

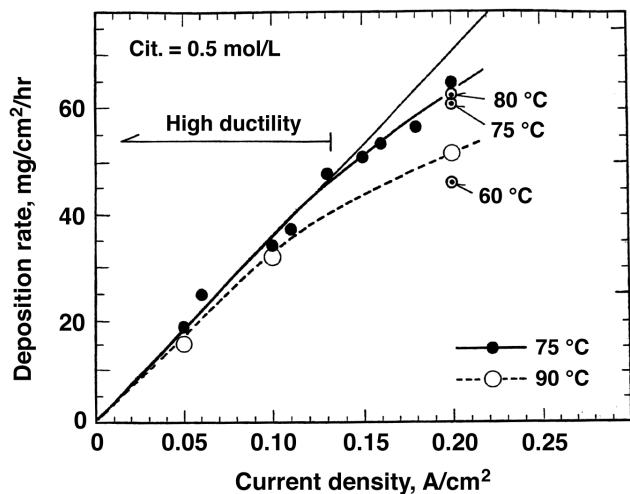


Fig. 5—Deposition rate vs. current density for electrodeposited Ni-W alloys for various plating bath temperatures between 60 and 90 °C at the trisodium citrate concentration of 0.5 mol/L.

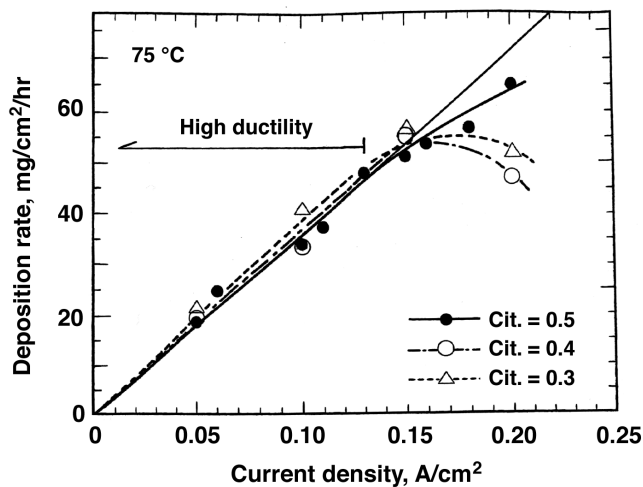


Fig. 6—Deposition rate vs. current density relationships for electrodeposited Ni-W alloys for various trisodium citrate concentrations between 0.3 and 0.5 mol/L at a plating bath temperature of 75 °C.

Table 2
Deposition Rate & Mechanical Properties vs.
Plating Bath Temperature For Ni-W Alloys
at a Current Density of 0.2 A/cm²

Plating Bath Temp °C	W Content at pct	Deposition rate mg/cm ² /hr	Vickers Hardness HV	Fracture Strain ϵ_f	Structure Judged by X-ray diff.
60	17.8	49.2	602	~0.00	nanocrystalline
70	19.9	65.0	650	0.02	nanocrystalline
75	22.5	68.8	685	1.00	amorphous
80	22.8	66.7	752	0.416	amorphous
90	25.0	55.1	770	0.005	amorphous

various current densities between 0.05 and 0.2 A/cm² at a plating bath temperature of 75 °C. X-ray diffraction peaks of the deposited alloys broadened and the tungsten content increased with increasing current density. The amorphous pattern again appeared at a tungsten content of about 20 at pct or more. Under these plating conditions, the Ni-W electrodeposits having amorphous and nanocrystalline structures were ductile: they could be bent through an angle of 180° without breaking ($\epsilon_f = 1.0$). Average grain sizes and Vickers microhardnesses of the as-deposited Ni-W alloys for various current densities between 0.05 and 0.2 A/cm² are collected in Table 3. Average grain sizes in the Ni-W electrodeposits were obtained by applying the Scherrer formula to the diffraction lines of fcc Ni (111) and the broad maximum of the

amorphous phase. With increasing current density, the average grain size decreased and the Vickers microhardness increased continuously. Upon annealing these materials at 450 °C for 24 hr, grain growth occurred in the range of 8.2 to 9.5 nm and the hardness was largely increased to more than HV = 900.

Figure 5 shows the relation between the deposition rate and the applied current density of the Ni-W electrodeposited alloys for various plating bath temperatures between 60 and 90 °C. Figure 6 displays the dependence of the deposition rate on the plating bath concentration of trisodium citrate at a bath temperature of

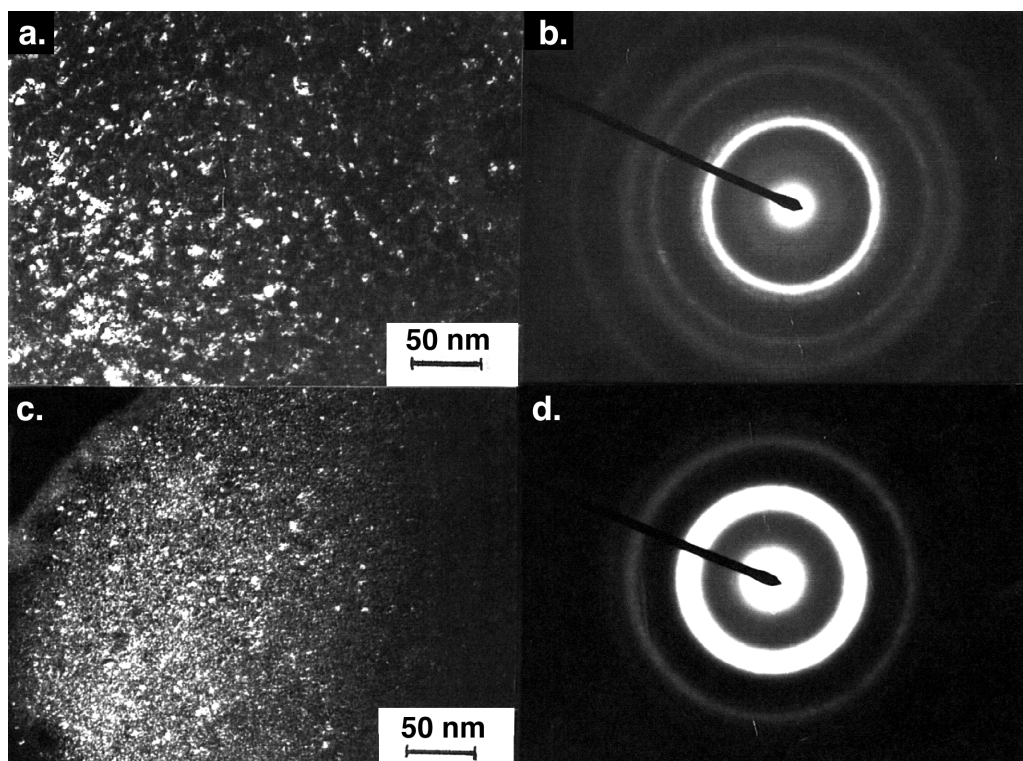


Fig. 7—Dark-field TEM images and selected area diffraction patterns in as-deposited Ni-W alloys at 75 °C: (a) and (b), Ni-17.7 at pct W alloy (0.05 A/cm²); (c) and (d), Ni-20.7 at pct W alloy (0.1 A/cm²).

Table 3
Average Grain Sizes & Vickers Microhardness
Of As-deposited Ni-W Alloys
Bath Temp 75 °C (450 °C for annealing 24 hr in vacuum)

Current Density 24 hr (A/cm ²)	W Content at. %	Grain Size		HV	
		as-deposited nm	as-deposited nm	Grain Size 450 °C, 24 hr	HV 450 °C, 24 hr
0.05	17.7	6.8	558	9.5	919
0.10	20.7	4.7	635	9.0	962
0.15	19.3	4.7	678	8.9	992
0.20	22.5	2.5	685	8.2	997

75 °C. The deposition rate increased linearly with increasing current density and then seemed to saturate. The saturation value of the deposition rate depended on plating bath conditions. As indicated in these figures, the ductile Ni-W electrodeposits were obtained for low current densities where the linear relationships holds between the deposition rate and the current density.

Structural Analysis of Ni-W Electrodeposits

Figure 7 shows the dark-field TEM images and the corresponding selected area diffraction patterns of the Ni-17.7 at pct W and the Ni-20.7 at pct W alloy electrodeposited with current densities of 0.05 A/cm² and 0.1 A/dm², respectively, at a plating bath temperature of 75 °C. In the case of the Ni-17.7 at pct W alloy, Figs. 5a and b, nanocrystalline structure was observed with grain sizes between five and eight nm. The selected area diffraction pattern revealed the fcc lattice Debye rings, indicating that the ultrafine grains were randomly oriented. In the case of the Ni-20.7 at pct W alloy, Figs. 5c and d, grain sizes of the nanocrystalline structure ranged between 2.5 and 3.5 nm. The selected area diffraction pattern consists only of amorphous-like halos. The high resolution fcc-(111) lattice image of this Ni-20.7 at pct W alloy having nanocrystalline structure with grain sizes between 2.5 and 3.5 nm is shown in Fig. 8. In the intercrystalline regions that are about 1 to 2 nm in width, distorted lattice images are observed. Similar features of HR-TEM observations have been observed in Ni-W alloys having grain sizes between 5 and 8 nm prepared by annealing the amorphous electrodeposited Ni-25.0 at pct W alloy.^{7,8}

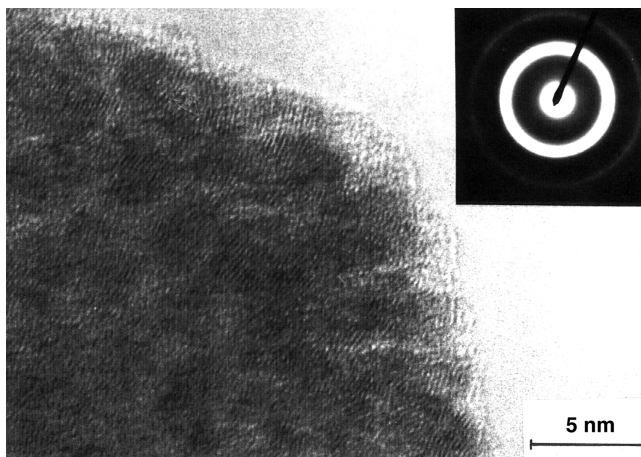


Fig. 8—High resolution fcc (111) lattice image showing 2.5 to 3.5 nm crystallites in as-deposited Ni-20.7 at pct W alloy using a current density of 0.1 A/cm² and its selected-area diffraction pattern.

Discussion

Brittleness of the As-Deposited Ni-W Alloys

It is well known that electrodeposited Ni-P amorphous alloys are severely brittle, whereas melt-quenched Ni-P amorphous alloys exhibit high ductility in bending tests. Suzuki *et al.*⁹ have reported that there were no significant differences of atoms and electronic structures between the electrodeposited and the melt-quenched Ni-P alloys, using X-ray and neutron diffraction techniques and have suggested that the brittleness of the electrodeposited Ni-P alloys may be caused by inclusion of hydrogen, water and anions in an electroplating solution during deposition. As indicated in Table 2, the amorphous electrodeposited Ni-22.5 at pct W alloy exhibiting high ductility was obtained at a plating bath temperature of 75 °C. At this temperature, the deposition rate (*i.e.*, the current efficiency for the deposition) of the Ni-W alloys reached its maximum value, indicating that the amount of codeposited hydrogen at the cathode during electrodeposition should be least. As also shown in Figs. 5 and 6, the ductile Ni-W electrodeposits were obtained in the region of low current densities where a linear relationship holds between deposition rate and current density. These results suggest that the ductile electrodeposits can be obtained under conditions where the amount of codeposited hydrogen is well diminished.

To clarify the effect of codeposited hydrogen on the brittleness, restoration behavior of the brittleness of the amorphous Ni-25.0 at pct W alloy, produced at a plating bath temperature of 90 °C and at an applied current density of 0.2 A/cm², was examined by measuring the fracture strain of the samples after annealing at various temperatures, the results of which are shown in Fig. 9. The fracture strain was measured by a simple bending test at room temperature. As shown, the fracture strains arise directly at the beginning of the annealing at 80, 90 and 200 °C, respectively, then slowly increase with increasing annealing time. These results support our assumption that the brittleness of the electrodeposited Ni-W alloys is caused mainly by inclusion of codeposited hydrogen. The effect of other factors on the brittleness such as an internal residual stress and inclusion of anions from the plating solutions are matters for future research.

The fracture strain was measured by a simple bending test at room temperature. As shown, the fracture strains arise directly at the beginning of the annealing at 80, 90 and 200 °C, respectively, then slowly increase with increasing annealing time. These results support our assumption that the brittleness of the electrodeposited Ni-W alloys is caused mainly by inclusion of codeposited hydrogen. The effect of other factors on the brittleness such as an internal residual stress and inclusion of anions from the plating solutions are matters for future research.

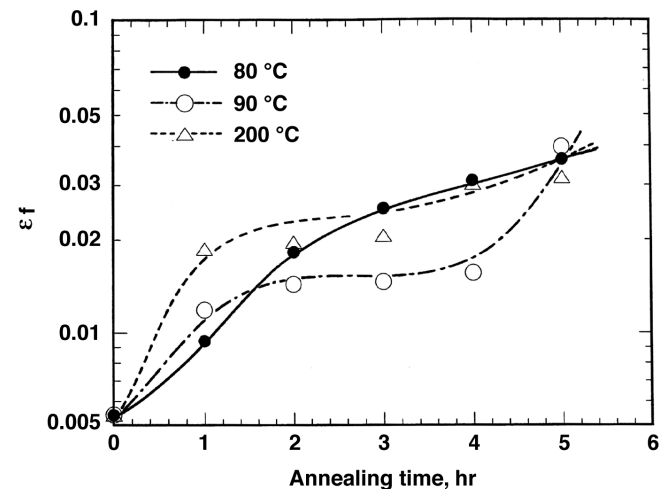


Fig. 9—Restoration behavior of the fracture strain as a function of annealing time at 80, 90 and 200 °C for Ni-25.0 at pct W alloy deposited at a plating bath temperature of 90 °C and at current density of 0.2 A/cm².

Hardness of the Nanocrystalline Ni-W Electrodeposits

In our previous studies,⁶⁻⁸ we have observed that the hardness of the nanocrystalline Ni-25.0 at pct W electrodeposited alloy decreased with decreasing grain size when the grain size was less than about 10 nm, and have proposed that this decrease in hardness may be a result of the increase of the intercrystalline volume fraction. With the Ni-20.7 at pct W alloy having grain sizes between 2.5 and 3.5 nm, shown in Fig. 6, the grain boundary thickness of 1 to 2 nm in widths evaluated from the HR-TEM observation may be considerably thicker than that of the coarse-grained materials. As a result, the volume fraction of the intercrystalline region in the Ni-W alloys should increase remarkably with decreased grain size. By annealing the Ni-W alloys, as indicated in Table 3, grain growth occurred and the hardness was largely increased. This increase in hardness may result from the decrease of the intercrystalline volume fraction.

Fujita¹⁰ has calculated the atomic structure of ultrafine crystallites on a nanometer scale by using a volume-free energy difference and the surface energy of an atomic cluster. The interface region of the nanocrystallites, having a structure of non-periodic atomic array, gradually expands into the center region when the size of crystallites decreases below a critical level. Van Swygenhoven *et al.*¹¹ have also calculated the influence of grain size of the mechanical properties of nanocrystalline Ni with grain sizes between 3 and 10 nm by a molecular dynamics computer simulation, and have proposed terms of grain boundary viscosity giving rise to a viscoelastic behavior with grain sizes below 5 nm. These results support the conclusion that the grain boundary thickness may increase with decreasing grain size, and the hardness of the expanded grain boundary region may be lower than that of the inner grain region.

Conclusions

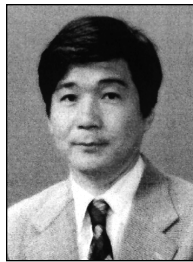
The amorphous and nanocrystalline Ni-W electrodeposited alloys having high hardness and high ductility with complete bending ($\epsilon_f = 1.0$) were obtained under plating conditions where the amount of codeposited hydrogen on the cathode is considerably diminished. It is suggested that the ductility of the Ni-W electrodeposited alloys may be strongly influenced by inclusion of the codeposited hydrogen during the electrodeposition process. By annealing the Ni-W electrodeposited alloys, grain growth occurred and the hardness was largely increased. This increase in hardness may be a result of the decrease of the intercrystalline volume fraction.

Editor's note: Manuscript received, November 1998.

References

1. W. Ehrfeld, V. Hessel, H. Löwe, Ch. Schulz & L. Weber, *Proc. 2nd Int'l Conf. Micro Materials '97*, Berlin, 112 (1997).
2. L.E. Vaaler & M.L. Holt, *J. Electrochem. Soc.*, **90**, 43 (1946).
3. L. Domnikov, *Metal Fin.*, **62**, 68 (1964).
4. G. Rauscher, V. Rogoll, M.E. Baumgärtner & Ch. J. Raub, *Trans. Inst. Metal Fin.*, **71**, 95 (1993).
5. N. Atanassov, K. Cencheva & M. Bratoeva, *Plat. and Surf. Fin.*, **84**, 67 (1997).
6. T. Yamasaki, W. Schneider, P. Schloßmacher & K. Ehrlich, *Proc. 2nd Int'l Conf. Micro Materials '97*, Berlin, 654 (1997).
7. T. Yamasaki, P. Schloßmacher, K. Ehrlich & Y. Ogino, *Materials Science Forum*, **269**, 975 (1998).
8. T. Yamasaki, P. Schloßmacher, K. Ehrlich & Y. Ogino, *NanoStructured Materials*, **10**, 375 (1998).

9. K. Suzuki, F. Itoh, T. Fukunaga & T. Honda, *Proc. 3rd Int'l Conf. on Rapidly Quenched Metals*, Brighton, **2**, 410 (1978).
10. H. Fujita, *Ultramicroscopy*, **39**, 369 (1991).
11. H. Van Swygenhoven & A. Caro, *Abstract of Int. Symp. on Metastable, Mech. Alloyed & Nanocrystalline Mater.*, (ISMANAM-97), Barcelona, (1997) 3/4-O-2.



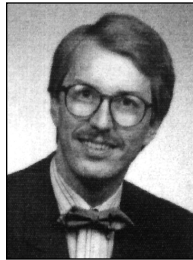
Yamasaki



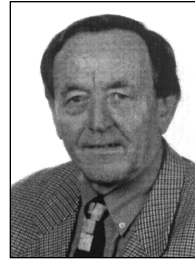
Tomohira



Ogino



Schloßmacher



Ehrlich

About the Authors

Dr. Tohru Yamasaki* is an associate professor in the Dept. of Materials Science & Engineering at the Himeji Institute of Technology, 2167 Shosha, Himeji, Hyogo 671-2201, Japan. He is responsible for materials design engineering. In 1995-96, he was a visiting scientist at the Institute of Materials Research at the Forschungszentrum Karlsruhe. He holds a PhD from the Himeji Institute of Technology, where his research activities are focused on structure and properties of amorphous and nanocrystalline materials produced by rapid quenching, mechanical alloying and electrodeposition.

Rika Tomohira is a graduate student at the Himeji Institute of Technology, where she received a B.Eng. degree. Her research is focused on formation of nanocrystalline metallic alloys by electrodeposition.

Dr. Yoshikiyo Ogino is a professor at the Himeji Institute of Technology, where he is responsible for materials design engineering. He is a graduate of Osaka University in metallurgy and holds a D. Eng from that institution. His research activities include structure and properties of nanocrystalline materials produced by non-equilibrium processes, such as mechanical alloying and electrodeposition.

Dr. Peter Schloßmacher studied physics at the University of Cologne and obtained a PhD from the RWTH Aachen. In 1991, he became a scientific staff member of the Institute of Materials Research at the Forschungszentrum Karlsruhe, where he is responsible for analytical and high-resolution transmission electron microscopy. His research activities include NiTi-based shaped memory alloys and electrodeposited metallic alloys for microsystems technology.

Dr. Karl Ehrlich is head of the Department of Physical Metallurgy and deputy director at the institute for Materials/ Nuclear Research Centre Karlsruhe. He holds a PhD from the Ludwig-Maximilian University of Munich and has published about 150 papers, mainly on materials for nuclear fission and fusion and, more recently, on materials for microsystem technology. He has been a member of advisory boards in many international conferences and is an acting member of the editorial advisory board of the *Journal of Nuclear Materials*.

* To whom correspondence should be addressed.